Atmos. Chem. Phys., 12, 6291–6307, 2012
www.atmos-chem-phys.net/12/6291/2012/
doi:10.5194/acp-12-6291-2012

Atmospheric Chemistry and Physics

Summertime weekly cycles of observed and modeled NO_x and O_3 concentrations as a function of satellite-derived ozone production sensitivity and land use types over the Continental United States

Y. Choi[1,2], **H. Kim**[1,2], **D. Tong**[1,2], **and P. Lee**[1]

[1]National Oceanic and Atmospheric Administration, Air Resources Laboratory, Silver Spring, MD 20910, USA
[2]Earth Resources Technology, Inc., Silver Spring, MD 20910, USA

Correspondence to: Y. Choi (yunsooc@gmail.com)

Received: 22 November 2011 – Published in Atmos. Chem. Phys. Discuss.: 18 January 2012
Revised: 22 June 2012 – Accepted: 27 June 2012 – Published: 19 July 2012

Abstract. To show how remote-sensing products can be used to classify the entire CONUS domain into "geographical regions" and "chemical regimes", we analyzed the results of simulation from the Community Multiscale Air Quality (CMAQ) model version 4.7.1 over the Conterminous United States (CONUS) for August 2009. In addition, we observe how these classifications capture the weekly cycles of ground-level nitrogen oxide (NO_x) and ozone (O_3) at US EPA Air Quality System (AQS) sites. We use the Advanced Very High Resolution Radiometer (AVHRR) land use dominant categories and the Global Ozone Monitoring Experiment-2 (GOME-2) $HCHO/NO_2$ column density ratios to allocate geographical regions (i.e., "urban", "forest", and "other" regions) and chemical regimes (i.e., "NO_x-saturated", "NO_x-sensitive", and "mixed" regimes). We also show that CMAQ simulations using GOME-2 satellite-adjusted NO_x emissions mitigate the discrepancy between the weekly cycles of NO_x from AQS observations and that from CMAQ simulation results. We found geographical regions and chemical regimes do not show a one-to-one correspondence: the averaged $HCHO\,/\,NO_2$ ratios for AVHRR "urban" and "forest" regions are 2.1 and 4.0, which correspond to GOME-2 "mixed" and "NO_x-sensitive" regimes, respectively. Both AQS-observed and CMAQ-simulated weekly cycles of NO_x show high concentrations on weekdays and low concentrations on weekends, but with one- or two-day shifts of weekly high peaks in the simulated results, which eventually introduces the shifts in simulated weekly-low O_3 concentration. In addition, whereas the high weekend O_3 anomaly is clearly observable at sites over the GOME-2 NO_x-saturated regime in both AQS and CMAQ, the weekend effect is not captured at sites over the AVHRR urban region because of the chemical characteristics of the urban sites ($\approx$ GOME-2 mixed regime). In addition, the weekend effect from AQS is more clearly discernible at sites above the GOME-2 NO_x-saturated regime than at other sites above the CMAQ NO_x-saturated regime, suggesting that the GOME-2-based chemical regime classification is more accurate than CMAQ-based chemical classification. Furthermore, the CMAQ simulations using the GOME-2-derived NO_x emissions adjustment (decreasing from 462 Gg N to 426 Gg N over the US for August 2009) show large reductions of simulated NO_x concentrations (particularly over the urban, or NO_x-saturated, regime), and mitigates the large discrepancies between the absolute amount and the weekly pattern of NO_x concentrations of the EPA AQS and those of the baseline CMAQ.

1 Introduction

Photochemical ozone (O_3) production near the earth's surface depends on the chemical environment, which is heavily influenced by the ratio of volatile organic compounds (VOCs) to nitrogen oxide ($NO_x = NO + NO_2$) emissions. While biogenic sources (vegetation) are primarily responsible for VOC emissions in many parts of the country, man-made sources contribute the majority of NO_x emissions in the United States (US). According to the US Environmental Protection Agency (US EPA), anthropogenic NO_x emissions in

the US are estimated to be 21.2 Tg per year (as in 2002): 38 % from on-road vehicles, 22 % from electric generation power plants, 22 % from off-road equipment, 11 % from commercial fuel combustion, and the rest from industrial processes and miscellaneous sources. Because of the dominance of mobile sources, NO_x emissions demonstrate a clear daily and weekly pattern related to temporal variations in the human use of fossil fuels. Therefore, an investigation of the daily or weekly variations of surface O_3 concentrations could illuminate the controlling effects of the key precursors of O_3 concentrations. Previous studies have focused on daily or weekly O_3 variations over several metropolitan areas, including New Jersey, Southern California, Los Angeles, Atlanta, Chicago, Denver, New York City, Dallas, Houston, Phoenix, Washington, DC, Baltimore, and their neighboring regions (e.g., Lebron, 1967; Cleveland et al., 1974; Elkus and Wilson, 1977; Vukovich, 2000; Marr and Harley, 2002; Fujita et al., 2003; Qin et al., 2004; Blanchard and Tanenbaum, 2006; Shutters and Balling Jr., 2006; Blanchard et al., 2008; Yarwood et al., 2008). These studies have highlighted the weekend effect on urban regions, where higher ground-level O_3 concentrations occur during the weekends rather than weekdays. However, the peaks of their precursors show an opposite trend: Higher urban region O_3 concentrations during the weekends are attributed to lower surface NO_x emissions in the NO_x-saturated environment.

The relationship between the weekly cycles of NO_x concentrations and emissions has been investigated utilizing remote sensing NO_2 column density products. For example, Beirle et al. (2003) and Kaynak et al. (2009) examined the weekly cycle of the NO_2 column density using retrieval products from the Global Ozone Monitoring Experiment (GOME) and the SCanning Imaging Absorption spectroMeter for Atmospheric CHartographY (SCIAMACHY), respectively, and found that temporal variations in the NO_x column density are proportional to emissions. In particular, Beirle et al. (2003) revealed a lower GOME NO_2 column density on weekends and a higher column density on weekdays over the US, European countries, Japan, and South Korea. Similarly, Kaynak et al. (2009) found relatively large SCIAMACHY NO_2 columns on weekdays and a significantly lower column density on weekends over polluted regions. However, no such large reduction has been found in rural areas. A strong correlation was also observed between the Ozone Monitoring Instrument (OMI)-derived surface NO_2 measurements and ground-based NO_2 measurements at the US Air Quality System (AQS) and Environment Canada's National Air Pollution Surveillance (NAPS) networks in polluted areas (Lamsal et al., 2008).

In addition to characterizing the weekly cycles of NO_x emissions, estimating a photochemical indicator, which is the ratio of VOCs to NO_x emissions, is crucial to a more thorough understanding of photochemical O_3 production because the photochemical environment strongly influences production. Sillman et al. (1990) and Sillman (1999) introduced a photochemical indicator that uses the ratios of certain chemical species to represent the O_3-NO_x-VOC sensitivity of a particular geographical area. Recently, Martin et al. (2004) and Duncan et al. (2010) utilized the ratio of satellite HCHO to the NO_2 column density from GOME (spatial resolution, 40 km × 320 km) and OMI (spatial resolution, 13 km × 24 km) as a photochemical indicator consistent with the ratio of VOCs to NO_x emissions over the surface. Martin et al. (2004) used the GOME-derived indicator to characterize geographic regions (e.g., North America, Europe, and East Asia) as chemical regimes (NO_x-saturated and NO_x-sensitive regimes). Using increased OMI-derived indicator, Duncan et al. (2010) found that most US cities had become more NO_x-sensitive regimes from 2005 to 2007.

Many previous studies (e.g., Lebron, 1967; Cleveland et al., 1974; Elkus and Wilson, 1977; Vukovich, 2000; Marr and Harley, 2002; Fujita et al., 2003; Qin et al., 2004; Blanchard and Tanenbaum, 2006; Shutters and Balling Jr., 2006; Blanchard et al., 2008; Yarwood et al., 2008) showed the weekly pattern of surface NO_x and/or O_3 over the AVHRR-derived US Geological Survey Land Use Land Cover (USGS LULC) regions (referred to as "AVHRR regions", which consist of urban, forest, and other regions) (Loveland et al., 2000) or GOME-2-derived chemical regimes (referred to as "GOME-2 chemical regimes", which are NO_x-saturated, NO_x-sensitive, and mixed regimes). Several other studies (e.g., Martin et al., 2004; Duncan et al., 2010) showed how remote sensing products can be used to determine the chemical environment. In this study, despite the uncertainty of remote sensing, we show that remote-sensing-derived chemical environments can be used for determining chemical regimes by directly showing the weekly cycles of surface O_3 from in-situ surface measurements over remote sensing-derived chemical regimes. No previous studies have addressed how the AVHRR-derived geographical regions can be chemically classified. This study investigates the chemical characteristics of AVHRR geographical regions by estimating the column ratios of GOME-2 formaldehyde (HCHO) to nitrogen dioxide (NO_2). In addition, two other previous studies (Kim et al., 2009; Russell et al., 2010) presented evidence of a large reduction in mobile source emissions over the western US or California since 1999 and since 2005. The reduction in point source emissions (e.g., from power plants) was accounted for during the preparation of the standard EPA National Emission Inventory 2005 (NEI 2005), but changes in mobile and other source emissions were not because of the lack of explicit data pertaining to changes over the entire CONUS domain. In this study, we perform two different CMAQ simulations – CMAQ simulation with NEI 2005 and CMAQ with GOME-2-derived NO_x emissions – to examine the impact of emissions changes on the weekly cycles of surface NO_x concentration.

To investigate the weekly cycles of surface O_3 concentrations at EPA AQS stations over different geographical regions and chemical regimes, we divide the 12 km CMAQ

model grids covering the CONUS into two different types of satellite-derived classifications: AVHRR-derived geographical regions and GOME-2-derived chemical regimes. We will also introduce CMAQ-derived chemical regimes (referred to as "CMAQ chemical regimes") to investigate the differences between the weekly cycles of surface O_3 concentrations at AQS stations of the GOME-2 and those of the CMAQ chemical regimes. Section 2 describes which measurement data are used for this study and then provides a description of the CMAQ 4.7.1 model. Section 3 briefly describes the methods used to define geographical regions and the GOME-2- and CMAQ-derived chemical regimes, and investigates variations in both the AQS-observed and CMAQ-simulated weekly cycles of daytime (01:00–05:00 p.m., local time) surface NO_x and O_3 concentrations at corresponding sites over AVHRR geographical regions and GOME-2 chemical regimes for August 2009 and the weekly cycles of NO_x and O_3 over GOME-2- and CMAQ-derived chemical regimes. In addition, Sect. 3 shows how CMAQ with GOME-2-derived emissions mitigate the discrepancies of the pattern of NO_x weekly cycles. Section 4 concludes and discusses the findings of this study.

2 Measurements and model

2.1 EPA air quality system (AQS) O_3 and NO_x

Hourly surface O_3 and NO_x concentrations are obtained from the EPA AQS measurement network (http://www.epa.gov/ttn/airs/airsaqs/detaileddata/downloadaqsdata.htm). Hourly-archived O_3 data from about 1100 measurement sites are utilized and mapped onto 12 km CMAQ model grid cells. The total number of CMAQ grids, including AQS O_3 measurement sites, is 874 (AVHRR urban, forest, and others), 897 (GOME-2 HCHO/$NO_2 < 1$: GOME-2 NO_x-saturated regime, $1 <$ GOME-2 HCHO/$NO_2 < 2$: mixed regime, GOME-2 HCHO/$NO_2 > 2$: NO_x-sensitive regime) and 875 (CMAQ HCHO/$NO_2 < 1$: CMAQ NO_x-saturated regime, $1 <$ CMAQ HCHO/$NO_2 < 2$: mixed regime, CMAQ HCHO/$NO_2 > 2$: NO_x-sensitive regime) (Table 1). Hourly-archived NO_x data from 265 measurement sites are utilized and mapped onto 227 model grids (AVHRR urban, forest, and other), 240 model grids (GOME-2 NO_x-saturated regime, mixed regime, NO_x-sensitive regime), and 234 model grids (CMAQ NO_x-saturated regime, mixed regime, NO_x-sensitive regime) (Table 1). We filtered out some data for the study of the weekly cycles of surface NO_x and O_3 because the weather conditions during the period of the remnant low of Tropical Storm Ana affecting the US (17–19 August 2009) produced large uncertainties regarding its meteorological impact on O_3 chemistry.

2.2 AVHRR USGS LULC data and GOME-2 NO_2 and HCHO column data

USGS LULC data are taken from the Global Land Cover Characteristics Data Base Version 2.0. A detailed description of the data is provided at http://edc2.usgs.gov/glcc/globdoc2_0.php. The 1 km-resolution AVHRR-derived global land cover characteristic data from the National Center for Earth Resources Observation and Science at USGS, the University of Nebraska-Lincoln, and the Joint Research Center of the European Commission (Loverland et al., 2000) were used to provide 24 types of land use and land cover information (Anderson et al., 1976). For this study, over the CONUS, AVHRR USGS LULC data are grouped into three categories (urban region: 1, forest regions: 11–15, other regions: all the rest except urban regions, forest regions, and water bodies) and then mapped onto 12 km CMAQ model grid cells following a Lambert conformal projection. A characteristic geographical region is determined based on the dominant land use type.

Remote sensing HCHO and NO_2 column densities are obtained from the retrieval products of the GOME-2 sensor, which is on board the EUMETSAT MetOp-A satellite. The instrument takes nadir measurements at 09:30 a.m. local time with footprints of $40 \times 80\,km^2$. OMI products (01:40 p.m., local time) are thought to be more suitable for determining chemical regimes, but a morning time satellite instrument is used in this study as it was in a previous study by Martin et al. (2004), mainly because consistent dynamical random errors have appeared since January 2009 in the OMI product (http://www.knmi.nl/omi/research/science/). Daily GOME-2 NO_2 and each orbit datum point of the HCHO column retrieval products are from http://www.temis.nl/airpollution. GOME-2 vertical NO_2 and HCHO column density data were prepared for a cell size of 0.25°, but some of the data were filtered out with a cloud fraction of $> 40\,\%$. Details pertaining to the NO_2 retrieval algorithm using the DOAS approach and error analysis are provided by Boersma et al. (2004). The retrieval data used in this study are obtained from the European Space Agency (ESA) Tropospheric Emission Monitoring Internet Service (TEMIS) (http://www.temis.nl/airpollution/no2.htm). A detailed description of the HCHO column product can be found in De Smedt et al. (2008). TM4NO2A version 2.1 is used for the GOME-2 NO_2 column density and TEMIS version 1.2 is for the GOME-2 HCHO column density.

2.3 Regional chemical transport model: CMAQ model version 4.7.1

CMAQ model version 4.7.1 (Foley et al., 2010) is configured with the Carbon Bond 2005 (CB05) chemical mechanism and AERO5 aerosol components. The CMAQ model runs are set up with a horizontal resolution of 12 km with 22 vertical layers from the surface reaching 100 hPa, derived

Table 1. The total number(one-month averages) of CMQ grids, including EPA AQS O_3 and NO_x measurement sites over the AVHRR-derived geographical regions, the GOME-2-derived chemical regimes, and the CMAQ-derived chemical regimes.

AVHRR-based	O_3 sites (874)	NO_x sites (227)	GOME-2-derived	O_3 sites (897)	NO_x sites (240)	CMAQ-derived	O_3 sites (875)	NO_x sites (234)
Urban	67	41	NO_x-saturated	58	34	NO_x-saturated	93	55
Others	535	138	Mixed	270	90	Mixed	236	91
Forest	272	48	NO_x-sensitive	569	116	NO_x-sensitive	546	88

by adapting a subset of the hybrid pure pressure and terrain-following σ-p coordinates of the Weather Research and Forecasting Non-hydrostatic Multi-scale Model dynamic core (WRF-NMM). The CMAQ vertical layer designation retains that of the WRF-NMM in the lower troposphere, specifically in the planetary boundary layer (Lee and Ngan, 2011). The CB05 (gas)-AQ (cloud)-AERO05 (aerosol) module in this model configuration considers O_3, PM, visibility, and acid deposition on the continental scale. The O_3 and $PM_{2.5}$ concentrations are driven by anthropogenic emissions based on the EPA National Emissions Inventory (NEI) for 2005. Wherever applicable, Continuous Emission Monitoring 2007 is used to replace the 2005 NEI for electric generating unit (EGU) point sources. Updated EGU emissions are further projected to 2009 using emission projection factors from the Department of Energy 2009 Annual Energy Outlook (AEO) report. All emissions independent from meteorological conditions are processed first using a modified version of the Sparse Matrix Operator Kernel Emission (SMOKE) model (Houyoux et al., 2000). The emission sectors that vary according to meteorological conditions are simulated with various emission models in the PRE-processor to CMAQ (PREMAQ). In this study, monthly mean lateral boundary conditions derived from the GEOS-CHEM (Bey et al., 2001) global model simulation results are used for August 2009, in light of the findings of earlier CMAQ evaluations that emphasized the drawback of using the climatologically-averaged static boundary condition (e.g., Tong and Mauzerall, 2006; Tang et al., 2008).

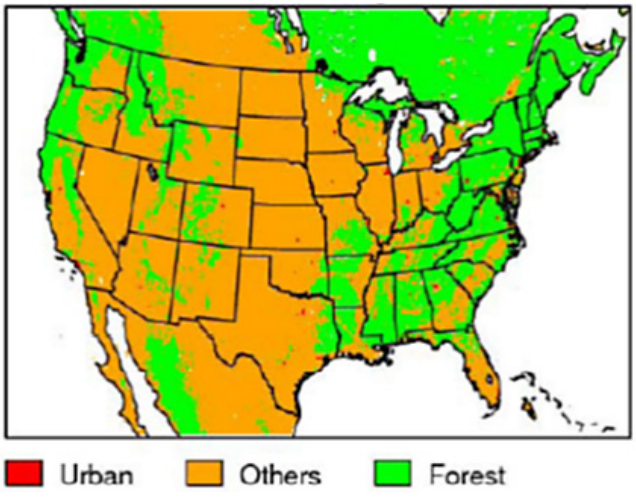

Fig. 1. Three AVHRR USGS LULC geographical regions (red: urban regions, including USGS LULC type 1; green: forest regions, including USGS LULC types 11–15; and orange: other regions, including all the rest except the urban region, the forest region, and water bodies (Anderson et al., 1976; Loverland et al., 2000).

3 Results

3.1 AVHRR geographical regions and GOME-2 and CMAQ chemical regimes

Previously, Kaynak et al. (2009) derived three geographical sites – urban, rural, and rural-point (rural areas, including large EGUs) – for their NO_x weekly cycle study. They chose seven urban sites based on Census 2000, eleven rural sites far from both urban regions and large EGUs, and more than 100 rural-point sites. In this study, instead of selecting specific sites, we divide the entire CONUS domain into three AVHRR-based geographical regions – urban, forest, and others (Fig. 1) – to examine how surface O_3 concentrations vary at all the available EPA AQS measurement sites over these geographical regions. Such a classification differs from that used in previous studies to characterize the weekly cycles of O_3, including the weekend effect in several urban regions (e.g., Cleveland et al., 1974; Elkus and Wilson, 1977; Vukovich, 2000; Marr and Harley, 2002; Fujita et al., 2003; Lebron, 2004; Qin et al., 2004; Blanchard and Tanenbaum, 2006; Shutters and Balling Jr., 2006; Blanchard et al., 2008; Yarwood et al., 2008). This study categories all of the model grid cells and EPA AQS measurement stations using a dominant AVHRR land use type. The AVHRR urban regions, which represent cities and their surrounding areas, comprise the smallest portion of the three geographical regions.

Previous remote sensing studies (e.g., Martin et al., 2004; Duncan et al., 2010) characterized two or three different regimes, including the NO_x-saturated/NO_x-sensitive and NO_x-saturated/mixed/NO_x-sensitive regimes. In this study, similar to Martin et al. (2004) and Duncan et al. (2010), we first utilize the ratio of GOME-2 HCHO to the NO_2 column density to divide the CONUS into three chemical regimes by using O_3 sensitivity derived from the GOME-2 ratio. Figure 2 represents the differences between the daytime (01:00–05:00 p.m., local time) surface O_3 of the baseline CMAQ and that of the CMAQ with a 30 % reduction in NO_x emissions

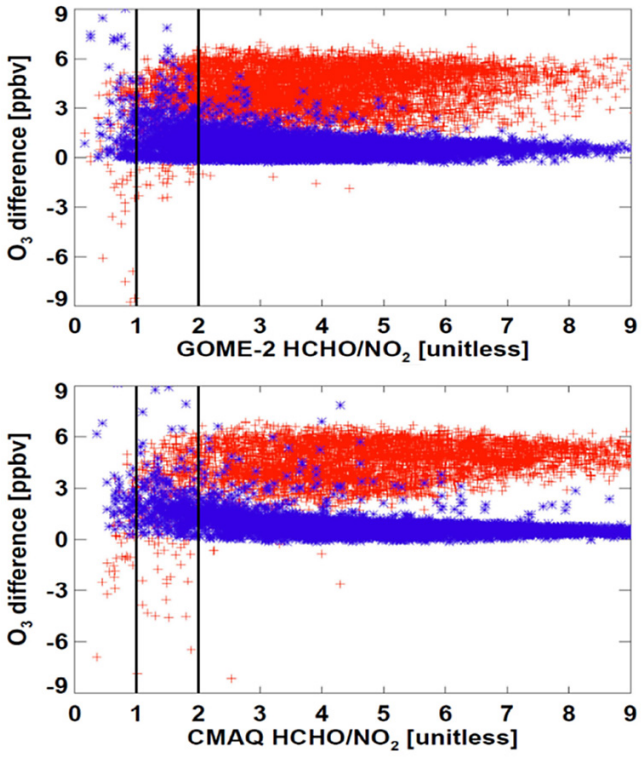

Fig. 2. Differences between the surface O_3 in the baseline CMAQ and that in CMAQ with 30 % NO_x reduction (in red, baseline – sensitivity) or a reduction in VOC emissions (in blue, baseline – sensitivity) in accordance with the ratios of the GOME-2 HCHO to NO_2 column density (upper panel) and the CMAQ HCHO to NO_2 column density (lower panel). The differences are estimated by averaging the data for the daytime (01:00–05:00 p.m., local time) during August 2009 only when GOME-2 NO_2 or the CMAQ NO_2 column density is larger than 1.0×10^{15} molecules cm^{-2}. So that the trend can be more clearly observable, all five O_3 differences are averaged according to the GOME-2 or CMAQ ratios.

(in red) and between CMAQ and CMAQ with a 30 % reduction in VOC emissions (in blue) in accordance with the ratio of GOME-2 or CMAQ HCHO to the NO_2 column density. No clear transitions take place among the NO_x-sensitive, mixed, and NO_x-saturated regimes, but changes in daytime surface O_3 are proportional to those in VOC emissions over the NO_x-saturated regime (for low HCHO / NO_2 ratio < 1), but surface O_3 is highly sensitive to changes in NO_x emissions over the NO_x-sensitive regime (for a high HCHO / NO_2 ratio of > 2). Over the mixed regime, some changes in surface O_3 are affected by those in VOC emissions, but more changes are affected by NO_x emissions changes (for ratios between 1 and 2). A high O_3 sensitivity to changes in NO_x emissions was similarly shown as the ratio of HCHO to the NO_2 column density increased, as was also shown in previous studies by Martin et al. (2004) and Duncan et al. (2010). The CONUS domain is divided into three chemical regimes using two transitions (ratios are 1 and 2, see Fig. 2). The left panel of Fig. 3 identifies three chemical regimes – NO_x-saturated, mixed, and NO_x-sensitive – using the transition. This study further categorizes other chemical regimes using the ratios of CMAQ HCHO to NO_2 column density (see the right panel of Fig. 3) to investigate how weekly cycles of NO_x and O_3 vary among the measurement stations of the GOME-2 and CMAQ chemical regimes of the CONUS. The CMAQ HCHO / NO_2 ratios are estimated at the GOME-2 overpass time.

Using one month-averaged GOME-2 NO_2 columns, some HCHO / NO_2 ratio data from CMAQ modeling grids are not considered when the NO_2 column density is less than 1×10^{15} molecules cm^{-2}, typical of regions remote to anthropogenic sources (e.g., Martin et al., 2006; Russell et al., 2010) (Fig. 3). The distribution of two different chemical regimes derived by GOME-2 and CMAQ is generally consistent over the CONUS, but with clear differences over some metropolitan areas (e.g., Houston, New Orleans, and Tampa, in Fig. 3). Thus, over such regions, another classification could introduce different surface O_3 sensitivity in model simulation. A zoomed-in regionalized study over the Southeastern US may highlight differences among these chemical regime definitions. In addition, NO_x-sensitive regimes (in red) from CMAQ are larger than those from GOME-2, implying higher surface O_3 sensitivity to changes in NO_x emissions in the model simulation.

We also analyze how the AVHRR geographical regions (e.g., urban, other and forest regions) represent the ratio of the GOME-2 HCHO / NO_2 columns (see Fig. 4). The GOME-2 HCHO / NO_2 mean values (standard deviations) of the AVHRR urban, other and forest regions are 2.1 (1.3), 3.8 (1.8), and 4.0 (1.9), respectively. A large variability implies that each geographical region could be classified as two or more chemical regimes. The GOME-2 HCHO/NO_2 mean values (standard deviations) of the GOME-2 NO_x-saturated, mixed, and NO_x-sensitive regimes are 0.6 (0.2), 1.6 (0.2), and 4.4 (1.6), respectively. The GOME-2 chemical ratios for the AVHRR urban and forest regions are 2.1 and 4.0, respectively, which likely correspond to those for the GOME-2 mixed (1.6) and NO_x-sensitive regimes (4.4), respectively. Interestingly, the chemical characteristic of the AVHRR urban regions is similar to that of the GOME-2 mixed regimes, which might affect the weekly cycle of the surface O_3 concentrations over the region. This issue will be described in detail in Sect. 3.4.

3.2 Weekly variation of NO_x emissions

To understand the weekly cycle of ground-level O_3 concentrations, we must evaluate weekly variations in the emissions of the O_3 precursor, NO_x. For the sake of consistency with the evaluation of the weekly O_3 cycle, only the daytime (01:00–05:00 p.m., local time) emissions from CMAQ is used. Large weekday/weekend variations in NO_x emissions are shown at EPA AQS stations over both the AVHRR

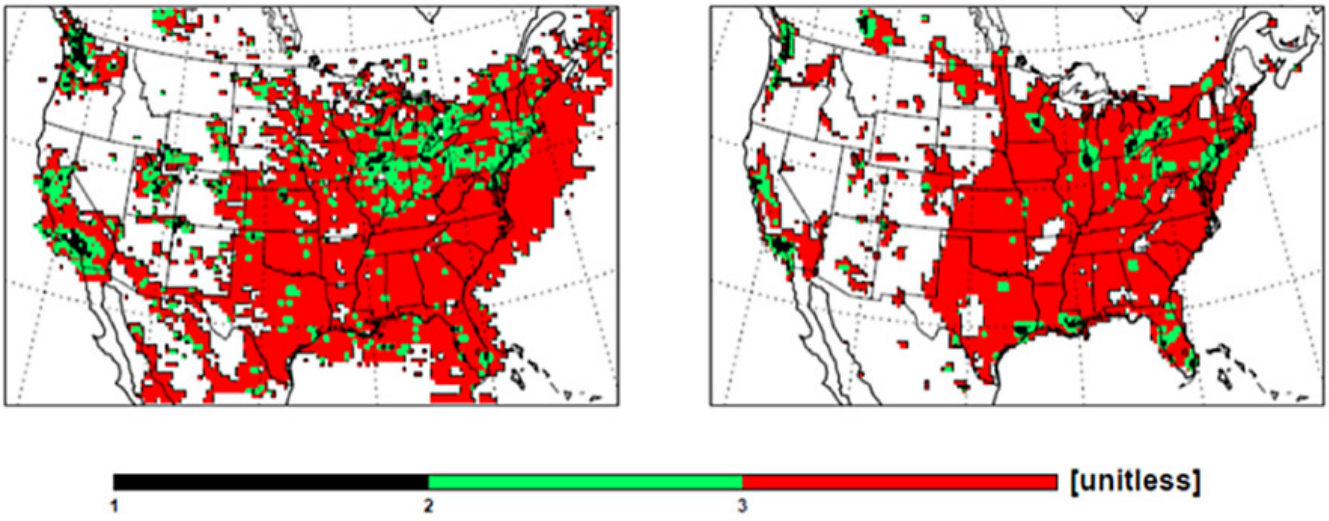

Fig. 3. Three GOME-2-derived and CMAQ-derived chemical regimes using two transitions (1 and 2, see Fig. 2) using the ratio of the GOME-2 HCHO to NO_2 (left panel) and the CMAQ HCHO to NO_2 column density (right panel). The CMAQ ratios are estimated at the overpass time. Black represents the category 1 region ($HCHO / NO_2 < 1$, an NO_x-saturated regime), green the category 2 region ($1 < HCHO / NO_2 < 2$, a mixed regime), and red the category 3 region ($HCHO / NO_2 > 2$, an NO_x-sensitive regime). The cell size of the GOME-2 HCHO and NO_2 column density data (from http://www.temis.nl/airpollution/) differs from that of CMAQ (12 km), and thus, both GOME-2 and CMAQ column density data are interpolated into 36 km for this comparison. Ratios are estimated only when the GOME-2 NO_2 column density is larger than 1.0×10^{15} molecules cm^{-2}.

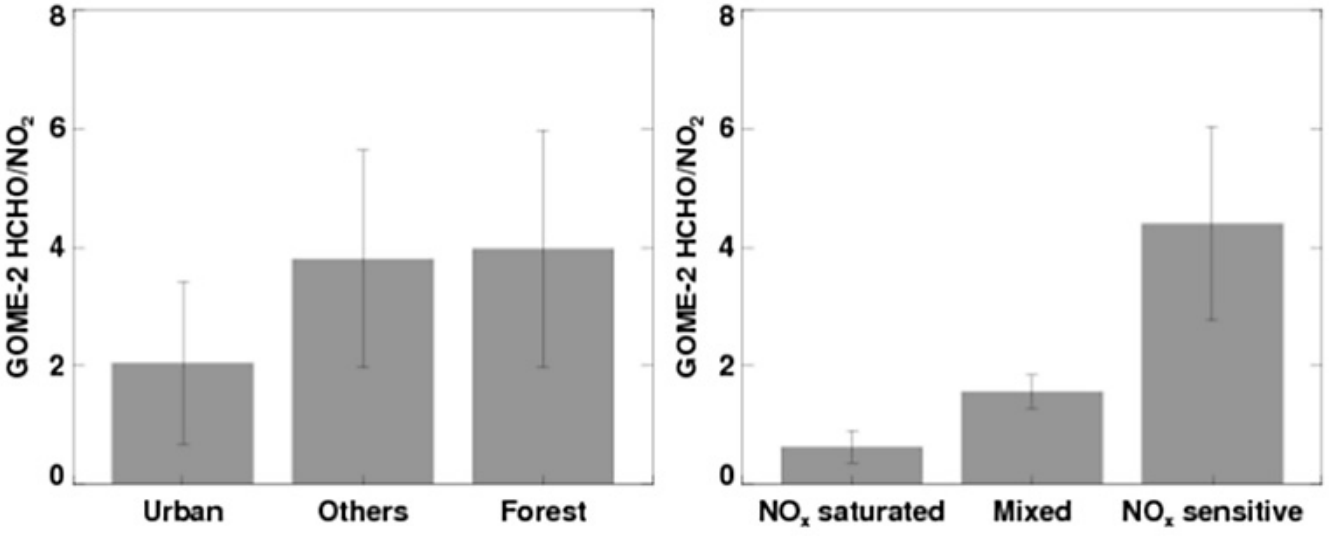

Fig. 4. The ratio of GOME-2 HCHO columns to NO_2 columns over AVHRR-derived geographical regions (i.e., urban, others, and forest regions, left panel) and GOME-2 derived chemical regimes (i.e., NO_x-saturated, mixed, and NO_x-sensitive regimes, right panel) for August 2009. The bar represents the standard deviation of GOME-2 $HCHO / NO_2$ ratio.

regions and the GOME-2 regimes (Fig. 5). Over the urban regions and the NO_x-saturated regimes, changes in weekday/weekend NO_x emissions are larger than those in other regions or regimes. From Friday to Saturday, NO_x emissions decrease by 29.4 %, 26.7 %, and 25.3 % over the urban, other, and forest regions, respectively. The reduction in NO_x emissions over the urban regions in this study is smaller than that in NO_x emissions (about 34 %) in the Los Angeles basin, estimated by Yarwood et al. (2008). Reductions are similarly estimated by 29.4 %, 26.6 %, and 26.4 % over NO_x-saturated, mixed, and NO_x-sensitive regimes, respectively. The greatest NO_x emissions are also shown on Friday over three AVHRR regions (7.76 mol s^{-1}, 1.94 mol s^{-1}, and 0.97 mol s^{-1}) and the GOME-2 regimes (5.25 mol s^{-1},

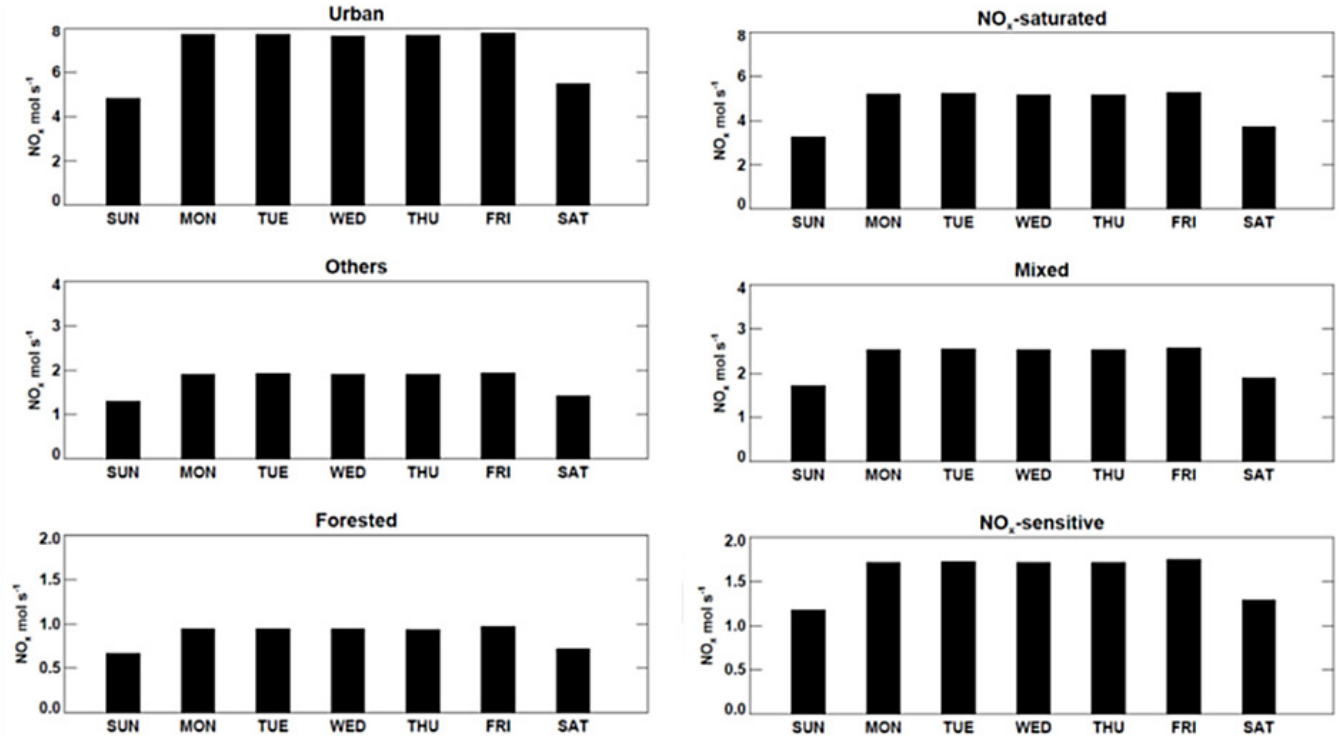

Fig. 5. Weekly variation in NO_X emissions at EPA AQS stations over three AVHRR-derived geographical regions (i.e., urban, other, and forest regions, left column) and GOME-2-derived chemical regimes (i.e., NO_X-saturated, mixed, and NO_X-sensitive regimes, right column) in CMAQ for August 2009. For the sake of consistency with the daytime O_3 comparison in Fig. 7, only daytime (01:00–05:00 p.m., local time) NO_X emissions are used; some data are filtered out from 17–19 August 2009, when Tropical Storm Ana strongly affected air quality over the eastern US.

2.57 mol s^{-1}, and 1.75 mol s^{-1}). Thus, changes in the absolute amounts of NO_X emissions over the urban regions from weekdays to weekends are larger than those over the NO_X-saturated regimes, but changes in NO_X emissions over the other and forest regions are smaller than those over the mixed and NO_X-sensitive regimes.

3.3 Weekly variation of AQS and CMAQ ground-level NO_x

We investigate weekly anomalies of ground-level AQS and CMAQ NO_X concentrations at EPA AQS stations over AVHRR geographical regions and GOME-2 chemical regimes, using only daytime (01:00–05:00 p.m., local time) observed and simulated NO_X concentrations and estimate weekly anomalies by subtracting averaged NO_X concentrations for each day from the average of all the available NO_X concentrations during the month over the urban, forest, and mixed regions (see the two left columns of Fig. 6) or the NO_X-saturated, mixed, and NO_X-sensitive regimes (see the two right columns of Fig. 6). For each day (from Sunday to Saturday), the number of data, the standard deviation, and the standard error of the mean (SEM) of AQS NO_X observations and corresponding CMAQ simulation results are also estimated (Table 2). The SEM is estimated the standard deviation dividing by the square root of the sample size (http://en.wikipedia.org/wiki/Standard_error), ranging from 0.1–0.9. The low weekend and high weekday NO_X is clearly observable at the stations located in all the AVHRR regions and GOME-2 regimes (Fig. 6). Over the urban regions and the NO_X-saturated regimes, AQS observations show the smallest NO_X concentrations during weekends (on Sunday) and the largest during weekdays (on Thursday and Friday). The weekly pattern of NO_X concentrations over urban regions is similar to that of the NO_2 column density and the NO_2 mixing ratio in previous studies (e.g., Beirle et al., 2003; Shutters and Balling Jr., 2006; Kaynak et al., 2009). In particular, Kaynak et al. (2009) showed the smallest NO_2 column density over the urban regions on Sunday and the largest on Wednesday, Thursday, and Friday (e.g., Wednesday for Chicago; Thursday for Houston, Atlanta, New York, and Phoenix; Friday for Los Angeles and Seattle). The CMAQ simulation shows a similar pattern for the smallest NO_X concentrations on Sunday and the largest on Thursday (over urban regions) and Wednesday (over NO_X-saturated regimes) instead of Friday, as in AQS. In general, the model-simulated NO_X peaks occur one or two days earlier than the AQS-observed NO_X peaks. Interestingly, the weekly pattern of the NO_X emissions inventory is not consistent with this simulated

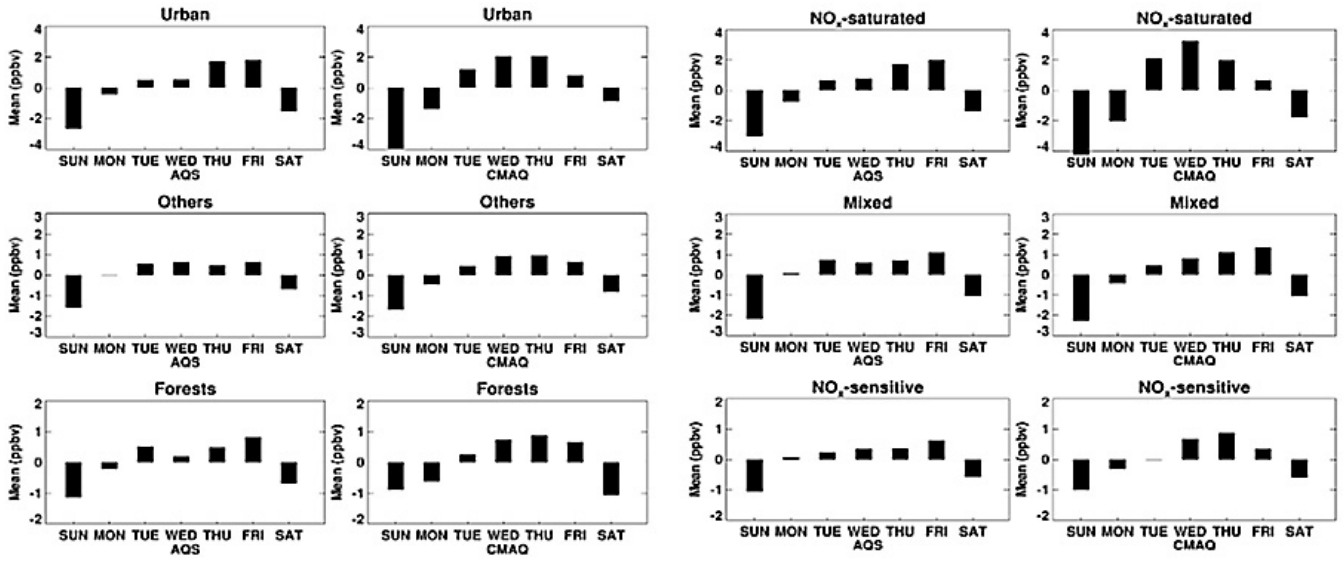

Fig. 6. Weekly anomalies of AQS-observed and CMAQ-simulated ground-level NO_x concentrations at EPA AQS stations over AVHRR-derived geographical regions (i.e., urban, other, and forest regions, left two columns) and GOME-2-derived chemical regimes (i.e., NO_x-saturated, mixed, NO_x-sensitive regimes, right two columns) for August 2009. For the sake of consistency with the daytime O_3 comparison in Fig. 7, only daytime (01:00–05:00 p.m., local time) NO_x concentrations are used; some data are filtered out from 17–19 August 2009, when Tropical Storm Ana strongly affected air quality over the eastern US.

NO_x pattern. Note that the NO_x emissions for Friday are slightly greater or similar to those for Wednesday over the regime or region (Fig. 5). However, the simulated NO_x concentrations significantly decrease from Wednesday to Friday over the regime or region, which introduces a large discrepancy between the weekday NO_x pattern of the model and that of the observation. The possible reason for this difference is described in Sect. 3.6. This shift in the highest NO_x day (Fig. 6) may contribute to the shift in the lowest O_3 day (Fig. 7), particularly at stations over urban regions or NO_x-saturated regimes because of the relatively greater amount of NO_x emissions than over other regions or regimes (Fig. 5). Details pertaining to the shifts in low O_3 peak days are described in the next section.

The weekly cycles of NO_x concentrations at AQS measurements sites over the AVHRR other region and GOME-2 mixed regimes in AQS are more or less similar to those in the AVHRR urban region and the GOME-2 NO_x-saturated regimes, respectively. CMAQ shows that the weekly cycle of NO_x concentrations at AQS sites over the AVHRR other region are similar to those over the AVHRR urban region. The simulated high-peak NO_x days (Tuesday–Thursday) over the NO_x-saturated regime shifted to late weekdays (Wednesday–Friday) over the mixed regime. In other words, although simulated weekly cycles of NO_x concentrations of urban and other regions are similar, simulated peak NO_x occurs two days later over mixed regimes than it does over NO_x-saturated regimes. Interestingly, the simulated NO_x cycle at AQS stations over mixed regimes is similar to the observed cycle at stations over NO_x-saturated regimes. It is most likely the result of the closeness of the mixed regime to the NO_x-saturated regime.

The AQS shows the largest NO_x concentration at stations over forest regions and NO_x-sensitive regimes on Friday, but CMAQ shows the largest NO_x concentrations in these areas on Thursday (Fig. 6). A study by Kaynak et al. (2009) also showed similar patterns of NO_2 column densities over their rural areas (large NO_2 column densities on Thursday and Friday and small column densities on Saturday and Sunday). The pattern of NO_x cycles at stations over the AVHRR forest regions in AQS and CMAQ is similar to that over the AVHRR other regions in AQS and CMAQ, respectively. Over forest regions and NO_x-sensitive regimes, the highest NO_x peak day occurs one day earlier in CMAQ (on Thursday) than in AQS (on Friday), which might be closely related to the one- or two-day shifts of low O_3 peak days during weekdays in CMAQ compared to those in AQS.

3.4 Weekly anomalies of AQS and CMAQ ground-level O_3

Weekly anomalies of ground-level O_3 concentrations from AQS and CMAQ are compared at EPA AQS measurement stations over the AVHRR geographical regions and the GOME-2 chemical regimes. Weekly O_3 anomalies and weekly NO_x anomalies are estimated in the same way. For each day, the number of data, the standard deviation and the SEM of AQS O_3 observations and corresponding CMAQ modeling results are also estimated (Table 3). Over urban

Table 2. The number of data (weekly anomaly), the standard deviation, and the standard error of the mean (SEM) of EPA AQS observations and CMAQ simulations for NO_x measurement sites over the AVHRR-derived geographical regions and the GOME-2-derived chemical regimes.

			AQS (NO_x)		CMAQ					AQS (NO_x)		CMAQ	
	Day	N	σ	$\sigma\ N^{-1/2}$	σ	$\sigma\ N^{-1/2}$		Day	N	σ	$\sigma\ N^{-1/2}$	σ	$\sigma\ N^{-1/2}$
Urban	SU	904	4.7	0.2	10.7	0.4	Saturated	SU	746	5.6	0.2	12.3	0.5
	MO	748	6.0	0.2	11.3	0.4		MO	616	7.6	0.3	14.1	0.6
	TU	554	6.5	0.3	14.5	0.6		TU	455	8.0	0.4	17.3	0.8
	WE	556	6.4	0.3	15.6	0.7		WE	453	7.6	0.4	18.7	0.9
	TH	749	7.7	0.3	14.2	0.5		TH	604	8.9	0.4	17.2	0.7
	FR	751	8.7	0.3	12.9	0.5		FR	613	9.4	0.4	15.2	0.6
	SA	886	5.6	0.2	13.9	0.5		SA	730	7.1	0.3	14.7	0.5
Others	SU	2940	3.1	0.1	7.2	0.1	Mixed	SU	2058	3.7	0.1	5.9	0.1
	MO	2453	5.1	0.1	7.9	0.2		MO	1665	7.0	0.2	8.2	0.2
	TU	1790	5.1	0.1	8.5	0.2		TU	1250	6.9	0.2	9.1	0.3
	WE	1833	5.5	0.1	9.2	0.2		WE	1246	6.9	0.2	9.5	0.3
	TH	2491	5.5	0.1	11.4	0.2		TH	1700	7.1	0.2	10.4	0.3
	FR	2516	5.5	0.1	10.0	0.2		FR	1688	7.2	0.2	11.3	0.3
	SA	2902	4.8	0.1	8.2	0.2		SA	2022	5.5	0.1	8.3	0.2
Forest	SU	1009	3.9	0.1	6.7	0.2	Sensitive	SU	2370	2.8	0.1	6.9	0.1
	MO	848	6.2	0.2	9.2	0.3		MO	2013	4.1	0.1	6.7	0.2
	TU	635	6.8	0.3	10.5	0.4		TU	1479	3.9	0.1	6.2	0.2
	WE	653	5.7	0.2	10.4	0.4		WE	1530	4.0	0.1	6.9	0.2
	TH	869	6.6	0.2	12.1	0.4		TH	2061	4.4	0.1	10.6	0.2
	FR	855	6.3	0.2	11.4	0.4		FR	2083	4.7	0.1	7.9	0.2
	SA	1006	5.7	0.2	7.6	0.2		SA	2364	4.0	0.1	7.3	0.2

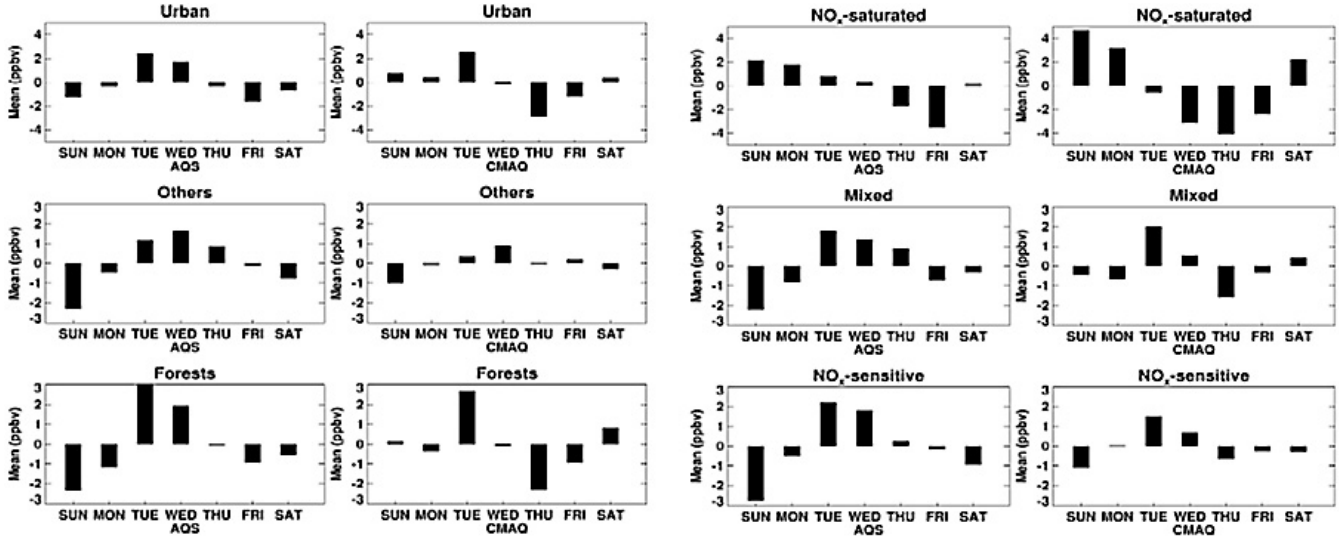

Fig. 7. The same as Fig. 6, but for ground-level O_3 concentrations.

regions, the largest observed ground-level O_3 concentrations occur on Tuesday, the same as those simulated by CMAQ (Fig. 7). The smallest O_3 concentrations occur on Friday in AQS, but on Thursday in CMAQ. The lowest O_3 days in AQS (on Friday) and CMAQ (on Thursday) correspond exactly to the highest NO_x days in the observation and the model, respectively. Figure 4 showed that the AVHRR urban regions are chemically classified as GOME-2 mixed regimes. Thus, interestingly, the weekly O_3 cycles over the AVHRR urban region from EPA AQS and CMAQ are similar to those over

Table 3. The number of data (weekly anomaly), the standard deviation, and the standard error of the mean (SEM) of EPA AQS observations and CMAQ simulations for O_3 measurement sites over the AVHRR-derived geographical regions and the GOME-2-derived chemical regimes.

			AQS (O_3)		CMAQ					AQS (O_3)		CMAQ	
	Day	N	σ	$\sigma\ N^{-1/2}$	σ	$\sigma\ N^{-1/2}$		Day	N	σ	$\sigma\ N^{-1/2}$	σ	$\sigma\ N^{-1/2}$
Urban	SU	1689	15.5	0.4	16.1	0.4	Saturated	SU	1426	21.2	0.6	20.2	0.5
	MO	1354	13.8	0.4	13.5	0.4		MO	1156	19.0	0.6	17.9	0.5
	TU	1014	14.8	0.5	16.6	0.5		TU	864	17.5	0.6	17.3	0.6
	WE	1023	16.7	0.5	16.5	0.5		WE	863	20.0	0.7	17.8	0.6
	TH	1366	17.1	0.5	17.6	0.5		TH	1149	21.5	0.6	18.2	0.5
	FR	1373	17.4	0.5	18.0	0.5		FR	1158	21.3	0.6	20.5	0.6
	SA	1686	16.9	0.4	19.4	0.5		SA	1404	21.8	0.6	23.8	0.6
Others	SU	13365	15.0	0.1	13.7	0.1	Mixed	SU	6716	15.9	0.2	14.8	0.2
	MO	10664	14.0	0.1	12.8	0.1		MO	5326	14.2	0.2	13.2	0.2
	TU	7961	14.6	0.2	13.3	0.1		TU	3990	14.7	0.2	13.5	0.2
	WE	8032	15.3	0.2	13.8	0.2		WE	4030	16.5	0.3	15.7	0.2
	TH	10690	16.2	0.2	15.0	0.1		TH	5381	16.8	0.2	16.0	0.2
	FR	10726	16.4	0.2	16.1	0.2		FR	5393	17.4	0.2	17.4	0.2
	SA	13183	15.5	0.1	15.3	0.1		SA	6645	17.4	0.2	17.3	0.2
Forest	SU	6826	14.0	0.2	12.8	0.2	Sensitive	SU	14318	13.0	0.1	12.3	0.1
	MO	5412	12.2	0.2	12.3	0.2		MO	11420	12.3	0.1	12.2	0.1
	TU	4038	13.3	0.2	12.6	0.2		TU	8524	13.8	0.1	13.2	0.1
	WE	4082	14.1	0.2	13.5	0.2		WE	8594	14.2	0.2	13.3	0.1
	TH	5434	15.3	0.2	14.8	0.2		TH	11432	14.9	0.1	14.9	0.1
	FR	5480	14.8	0.2	14.7	0.2		FR	11488	15.0	0.1	15.1	0.1
	SA	6797	14.4	0.2	14.0	0.2		SA	14230	13.7	0.1	13.7	0.1

the GOME-2 mixed regimes (Fig. 7). Blanchard et al. (2008) showed three different high O_3 peak days (on Sunday in Chicago, Dallas-Fort Worth, and Phoenix for all O_3 season days; on Tuesday in Chicago and Phoenix for high O_3 days; and on Saturday in Dallas-Fort Worth for high O_3 days). Their study found that over several urban sites for high O_3 days, the highest O_3 peak days occur on Tuesday. From another study by Shutter and Balling Jr. (2006), high O_3 peak days in Phoenix occur on Sunday. Interestingly, in our study, the highest O_3 peak day over the NO_x-saturated regime is Sunday. The study by Blanchard et al. (2008) also showed various low peak days (on Monday in Chicago for high O_3 days; on Wednesday in Phoenix for all O_3 season days; on Thursday in Dallas-Fort Worth, Dallas-fort Worth , and Phoenix for high O_3 days; and on Friday in Chicago for all O_3 seasonal days). Our study shows that the lowest O_3 peak days occur on Fridays (in AQS) and Thursdays (in CMAQ) over both urban regions and NO_x-saturated regimes. A previous study by Blanchard et al. (2008) showed more diverse highest and lowest peak days than our study, likely resulting from the local characteristics of the measurement sites.

Previous studies clearly showed the weekend effect in several polluted areas (e.g., Cleveland et al., 1974; Elkus and Wilson, 1977; Vukovich, 2000; Marr and Harley, 2002; Fujita et al., 2003; Lebron, 2004; Qin et al., 2004; Shutter and Balling Jr., 2006; Yarwood et al., 2008), but this study finds no weekend effect at AQS stations over the AVHRR urban regions in AQS nor in CMAQ because the AVHRR urban region has a similar chemical environment to the GOME-2 mixed regime, instead of the GOME-2 NO_x-saturated regime. However, at other AQS sites over NO_x-saturated regimes, the weekend effect is clearly shown in both AQS and CMAQ, indicating a peak ground-level O_3 concentration on Sunday both in AQS and CMAQ. Both AQS and CMAQ also show the second highest peak on Monday. At AQS stations over NO_x-saturated regimes, AQS observations indicate the smallest O_3 on Friday, but the CMAQ simulation shows the smallest on Thursday (see Fig. 7). The difference between the observed and simulated lowest O_3 days is most likely the result of temporal variations of NO_x concentrations over the regime (see Fig. 6).

At AQS stations over the AVHRR other regions, the largest and smallest O_3 concentrations are shown on Wednesday and Sunday, respectively. The CMAQ model simulation results show the same highest and lowest O_3 days. Both AQS and CMAQ show negative anomalies on Saturday (Fig. 7), which are consistent with negative anomalies in NO_x concentrations (Fig. 6). At AQS sites over the mixed regime, both the AQS observation and the CMAQ simulation show the largest O_3 concentrations on Tuesday. The AQS observation shows

the smallest O_3 concentrations on Sunday, but the CMAQ simulation shows the smallest on Thursday. The reason for negative anomalies on Thursday and Friday in CMAQ is not clear, but the AQS observation also shows similar negative anomalies on Friday and Saturday. As we explained earlier, the differences between the lowest O_3 days in AQS and those in CMAQ are similarly shown over the AVHRR urban region. Similarly, the low O_3 peak day occurs one day earlier in CMAQ (Thursday) than in AQS (Friday) during the weekdays. The transport of small O_3 concentrations over NO_x-saturated regimes might introduce small O_3 concentrations over its neighboring mixed regime. At AQS stations over forest regions, both AQS and CMAQ show the largest O_3 concentrations on Tuesday, but they show the smallest on Sunday or Thursday, respectively. At AQS stations over NO_x-sensitive regimes, both AQS and CMAQ show the largest O_3 concentrations on Tuesday, the second largest on Wednesday, and the smallest on Sunday. The highest O_3 peak day over the NO_x-sensitive regime is similar to that of the AVHRR forest region, likely due to the similar chemical environment of the regime to that of the region (Fig. 4).

3.5 Weekly anomalies of NO_x and O_3 over the CMAQ chemical regimes

In this section, we further investigate the effects of the difference between the GOME-2- and CMAQ-derived chemical regimes (see Fig. 3) on weekly cycles of surface NO_x and O_3 concentrations at AQS measurement station sites. This study compares the weekly NO_x and O_3 cycles at the AQS stations over the two different NO_x-saturated regimes (from GOME-2 and CMAQ). The weekly cycles of NO_x at corresponding stations in AQS and CMAQ over the two different chemical regimes (see the two right columns of Fig. 6 and the two left columns of Fig. 8) are generally similar. Table 4 represents the number of data, the standard deviation, and the SEM of AQS NO_x or O_3 observations and corresponding CMAQ simulation results at AQS stations over the CMAQ-derived chemical regimes. As discussed in the previous section, the O_3 weekend effect in AQS and CMAQ (see the two right columns of Fig. 7) are clearly observable at AQS stations over the GOME-2 NO_x saturated regime, but high O_3 anomalies on Sunday and Monday are not obvious at AQS stations over the CMAQ NO_x saturated regime in AQS (see the third column of Fig. 8). Interestingly, the pattern of weekly O_3 cycles over the CMAQ NO_x-saturated regime is similar to that over the AVHRR urban region (see the first column of Fig. 7). This finding indicates that CMAQ-derived NO_x-saturated regime stations might be characterized as AVHRR urban region stations that, in reality, include some AVHRR urban region stations. This finding further suggests that utilizing the GOME-2-derived photochemical indicator might define NO_x-saturated regime stations better than the CMAQ-derived photochemical indicator.

3.6 The impact of the GOME-2-derived emissions inventory on the weekly NO_x pattern

As we described in Sect. 2.2, GOME-2 NO_2 retrievals were obtained for August 2009 and used to calculate monthly-averaged NO_2 column density for the CONUS domain, and an equivalent monthly mean column-integrated value of NO_2 concentrations was calculated from the CMAQ with NEI 2005. The ratios of the CMAQ NO_2 column density to the GOME-2 NO_2 column density are also estimated (Fig. 9). A comparison of modeled and satellite-observed NO_2 columns exhibited general overestimates in urban areas close to concentrated population areas over the CONUS. In particular, the CMAQ model over-predicted the NO_2 column density in the urban areas over Houston, Texas, New Orleans, Louisiana, Tampa and Jacksonville, Florida, Portland, Oregon, Minneapolis, Minnesota, Tulsa, Oklahoma, Kansas City, Kansas, Charlotte and Raleigh, North Carolina, and Los Angeles, California. Even though other regions exhibited various prediction trends, Martin et al. (2006) and Choi et al. (2008, 2009) also showed similar over-prediction trends of the GEOS-CHEM model (using NEI1999) and the Regional chEmical trAnsport Model (REAM) model (using NEI 1999 or NEI 1999 with a 50 % reduction in EGU and non-EGU point sources, respectively) in urban areas over the southern US.

Unlike in the results discussed in the previous paragraph, the baseline model generally underpredicts NO_2 column density in areas near San Francisco, California, Springfield, Illinois, Bloomington, Indiana, Binghamton, New York, and Scranton, Pennsylvania, and large portions of rural area over the CONUS (Fig. 9). Napelenok et al. (2008) also showed that NO_2 column densities are generally underpredicted in rural areas over the eastern US in the baseline CMAQ model. Interestingly, over San Francisco and its neighboring region, the GEOS-Chem (Martin et al., 2006) and the REAM (Choi et al., 2008, 2009) CTMs also showed underprediction of the NO_2 columns.

To analyze the effect of the GOME-2-derived emissions inventory on the weekly cycles of surface NO_x over the AVHRR geographical regions or the GOME-2 chemical regimes, we performed additional simulations, including the GOME-2-derived NO_x fossil-fuel emissions. The GOME-2-derived NO_x fossil-fuel emissions inventory (E_t) is first estimated following Martin et al. (2003) and Choi et al. (2008) by fitting E_t to a priori bottom-up emission E_a from NEI 2005 with the ratio of the retrieved NO_2 column (Ω_r) to the corresponding simulated column at the GOME-2 overpass time (Ω_s):

$$E_t = E_a \times \Omega_r / \Omega_s \quad (1)$$

For a new emissions inventory, we estimated the ratios of the CMAQ NO_2 column density to the GOME-2 NO_2 column density. For this application, we estimated both the ratios of the CMAQ NO_2 columns to GOME-2 NO_2 columns

Table 4. The number of data (weekly anomaly), the standard deviation, and the standard error of the mean (SEM) of EPA AQS observations and CMAQ simulations for NO_x and O_3 measurement sites over the CMAQ-derived chemical regimes.

			AQS (NO_x)		CMAQ				AQS (O_3)		CMAQ	
	Day	N	σ	$\sigma\ N^{-1/2}$	σ	$\sigma\ N^{-1/2}$	Day	N	σ	$\sigma\ N^{-1/2}$	σ	$\sigma\ N^{-1/2}$
Saturated	SU	1253	5.0	0.1	12.1	0.3	SU	2317	21.2	0.4	19.1	0.4
	MO	1033	8.2	0.3	13.8	0.4	MO	1871	19.0	0.4	16.1	0.4
	TU	762	8.3	0.3	15.7	0.6	TU	1407	17.7	0.5	15.8	0.4
	WE	758	7.7	0.3	16.7	0.6	WE	1412	20.2	0.5	17.1	0.5
	TH	1025	8.7	0.3	18.4	0.6	TH	1886	20.8	0.5	17.9	0.4
	FR	1029	9.0	0.3	16.0	0.5	FR	1883	20.9	0.5	20.2	0.5
	SA	1219	7.0	0.2	14.0	0.4	SA	2299	20.8	0.4	22.0	0.5
Mixed	SU	2031	3.3	0.1	5.1	0.1	SU	5892	14.5	0.2	14.9	0.2
	MO	1636	5.4	0.1	5.5	0.1	MO	4686	13.7	0.2	13.6	0.2
	TU	1203	5.3	0.2	5.2	0.1	TU	3509	15.6	0.3	15.4	0.3
	WE	1219	5.8	0.2	6.1	0.2	WE	3535	16.1	0.3	15.8	0.3
	TH	1653	6.1	0.2	8.2	0.2	TH	4703	16.7	0.2	16.6	0.2
	FR	1652	6.3	0.2	7.3	0.2	FR	4732	16.6	0.2	17.2	0.3
	SA	1989	4.5	0.1	6.9	0.2	SA	5863	16.2	0.2	16.6	0.2
Sensitive	SU	1724	3.0	0.1	3.1	0.1	SU	13687	13.6	0.1	12.4	0.1
	MO	1503	4.0	0.1	3.3	0.1	MO	10888	12.4	0.1	12.0	0.1
	TU	1120	3.8	0.1	3.9	0.1	TU	8118	13.1	0.1	12.1	0.1
	WE	1148	3.8	0.1	4.8	0.1	WE	8194	14.1	0.2	13.0	0.1
	TH	1563	3.9	0.1	5.0	0.1	TH	10913	14.9	0.1	14.4	0.1
	FR	1558	4.7	0.1	4.8	0.1	FR	10965	15.2	0.1	14.9	0.1
	SA	1739	4.6	0.1	4.3	0.1	SA	13553	14.3	0.1	14.0	0.1

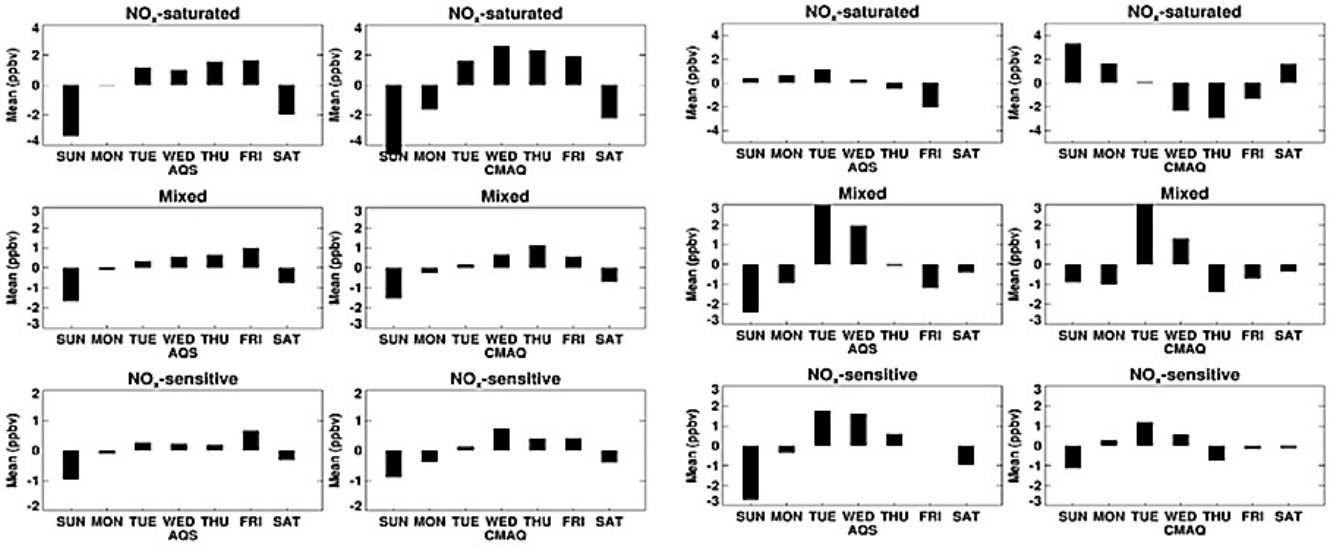

Fig. 8. Weekly anomalies of AQS-observed and CMAQ-simulated ground-level NO_x at EPA AQS NO_x stations (left two columns) and O_3 concentrations at EPA AQS O_3 stations (right two columns) over CMAQ-derived chemical regimes (i.e., NO_x-saturated, mixed, and NO_x-sensitive regimes, see the right panel of Fig. 3) for August 2009. Only daytime (01:00–05:00 p.m., local time) NO_x and O_3 concentrations are used; some data are filtered out from 17–19 August 2009, when Tropical Storm Ana strongly affected air quality over the eastern US.

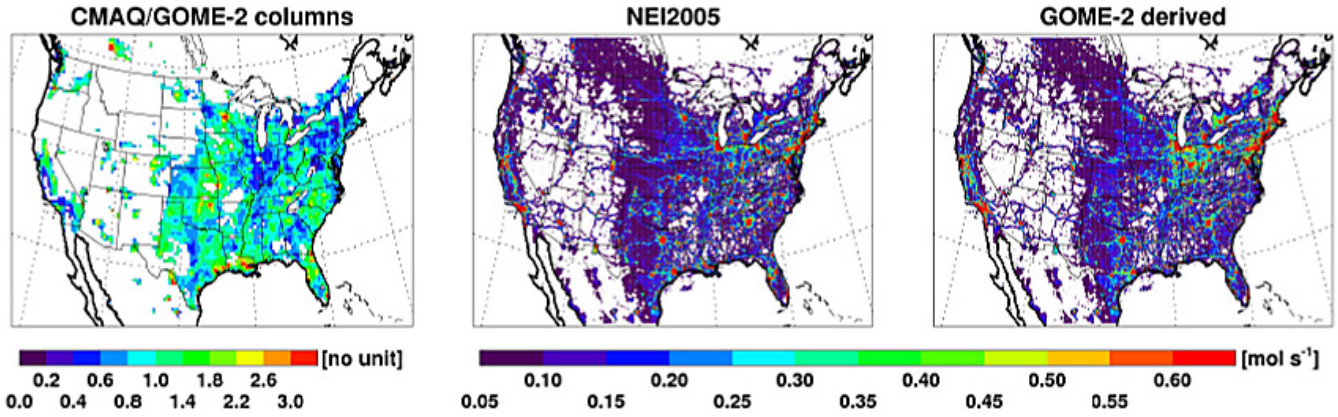

Fig. 9. The ratio of the monthly-averaged CMAQ NO_2 columns versus GOME-2 NO_2 columns (left panel, both GOME-2 and CMAQ column data are interpolated for 36 km for this comparison), the monthly-averaged NO_x emissions from EPA National Emissions Inventory 2005 (NEI 2005, middle panel, 462 Gg N over the US) and the monthly-averaged NO_x emissions from the GOME-2-derived emissions inventory (right panel, 426 Gg N over the US) for August 2009.

in a 36 km spatial resolution in order to effectively avoid the adverse effect of the transport of NO_2 tracers in a fine resolution and the GOME-2-derived NO_x emissions inventory by applying the ratios to the standard NEI 2005 (Fig. 9). The GOME-2-derived NO_x emissions (426 Gg N) are 7.8 % less than the NEI 2005 (462 Gg N) emissions over the US (Fig. 9).

Figure 10a and b show a comparison of the simulated surface NO_x concentrations from the CMAQ with NEI 2005 and the second CMAQ with the GOME-2-derived emissions inventory. The simulated NO_x concentrations from the second CMAQ are significantly less at EPA stations, particularly over the AVHRR urban region and the GOME-2 NO_x-saturated regime (Fig. 10a and b). The number of available AQS data, the standard deviations and the SEM of corresponding CMAQ simulation results with GOME-2-derived emissions are estimated (Table 5). Interestingly, the standard deviation and the SEM values from the 2nd CMAQ simulations become similar to those from the AQS observations. We also found that the large reduction in NO_x emissions affects the weekly pattern of surface NO_x at stations over the urban region or the NO_x-saturated regime (Fig. 10a and b). As we described earlier, the CMAQ-simulated NO_x peak days occur in one- or two-day shifts compared with those from the EPA AQS observations (Fig. 6). The trend in weekly NO_x emissions (see Fig. 5) reveals similar emissions from Monday to Friday, but the standard CMAQ shows a peak NO_x day on Wednesday. The simulated high peak occurrence on Wednesday is probably related to the longest NO_x lifetime in the middle of the week, which could be caused by the overestimated surface NO_x concentrations or favorable meteorological condition for NO_x tracers on Wednesday in CMAQ. The details need to be further investigated. Note that large reductions in NO_x emissions mitigate rapid changes in simulated NO_x concentration (an increase from Monday to Wednesday and a decrease from Wednesday to Friday) during the weekdays at stations over the urban region or the NO_x-saturated regime (see the second and third columns of Fig. 10a and b).

4 Conclusion and discussion

This study compares the weekly cycles of surface ozone and its precursors simulated by the CMAQ model to that observed at the EPA AQS stations over satellite derived geographical regions and chemical regimes over the contiguous United States. We found that the CMAQ model generally captures the weekly cycles of ground-level NO_x and O_3 as observed at AQS sites, except occasional shifts between positive and negative anomalies during weekdays. Over AVHRR other and forest regions and GOME-2 mixed and NO_x-sensitive regimes, both AQS and CMAQ show positive NO_x anomalies during weekdays and negative NO_x anomalies during weekends. Similarly, AQS and CMAQ show negative O_3 anomalies during weekends and positive O_3 anomalies during weekdays. However, AQS observations do not reveal any weekend effects (high O_3 weekly anomalies during weekends) at AQS stations over the AVHRR urban region, but they clearly show weekend high O_3 anomalies at other AQS stations over the GOME-2 NO_x-saturated regime, suggesting that characterizing the CONUS as GOME-2 chemical regimes could benefit the analysis of weekly cycles (including the weekend effect). Over the AVHRR urban region and the GOME-2 NO_x-saturated regime, the greatest negative O_3 day differs slightly in AQS (on Friday) and CMAQ (on Thursday). A shift in the largest negative O_3 anomaly day in CMAQ is likely to result from a shift in the positive NO_x day in the model, unlike shifts in AQS. Compared to GOME-2 NO_2 column in August 2009, the CMAQ NO_2 column is generally larger, particularly over the AVHRR urban region and NO_x-saturated regime. Adjusting fossil-fuel NO_x emissions (from 462 to 426 Gg N over the US) based on a

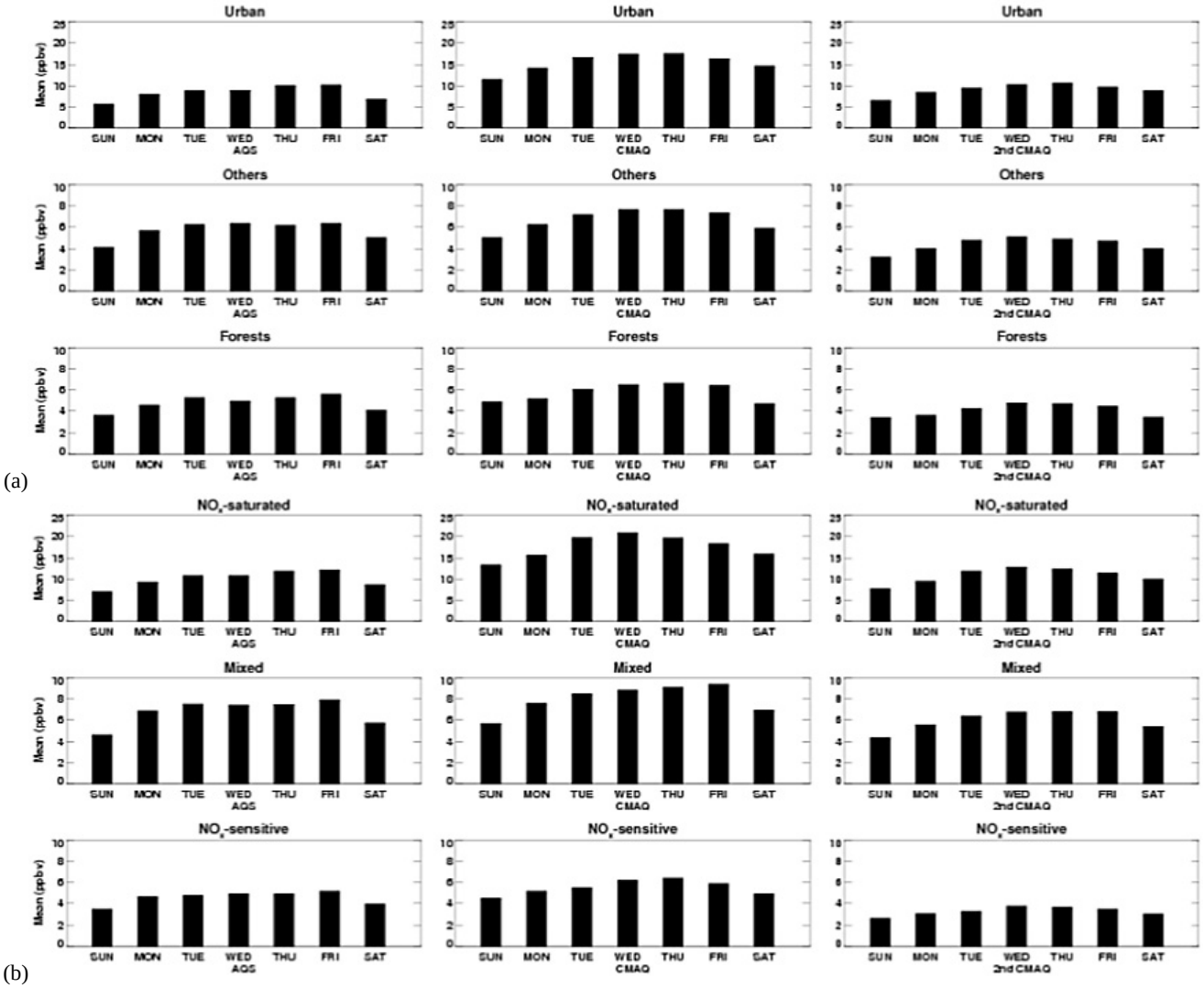

Fig. 10. (a) Weekly mean variations of AQS-observed, CMAQ-simulated, and the 2nd CMAQ-simulated (with GOME-2-derived emissions inventory) ground-level NO_X concentrations at EPA AQS stations over AVHRR-derived geographical regions (i.e., urban, other, and forest regions) for August 2009. For the sake of consistency with the daytime O_3 comparison in Fig. 7, only daytime (01:00–05:00 p.m., local time) NO_X concentrations are used; some data are filtered out from 17–19 August 2009, when Tropical Storm Ana strongly affected air quality over the eastern US. Note that the index of the vertical y-axis for the urban region stations (0–25 ppbv) differs from the indices (0–10 ppbv) of other and forest region stations. **(b)** Same as in **(a)**, but over GOME-2-derived chemical regimes (i.e., NO_X-saturated, mixed, NO_X-sensitive regimes). Note that the index of the vertical y-axis for NO_X-saturated regime stations (0–25 ppbv) differs from the indices (0–10 ppbv) of mixed and NO_X-sensitive regime stations.

comparison of CMAQ and GOME-2 NO_2 columns proves to reduce the large discrepancy in the absolute amounts of surface NO_X concentrations and the weekly pattern of surface NO_X concentrations between CMAQ and EPA AQS, in particular over the AVHRR urban region and the GMOE-2 NO_X saturated regime.

This study also analyzes and compares the weekly cycles of NO_X and O_3 over the two different chemical regimes from GOME-2 and CMAQ. A weekend effect is clear at AQS stations over the GOME-2-derived NO_X-saturated regime, but it is not at other AQS stations over the CMAQ-derived NO_X-saturated regime. After selecting a specific region of interest as a chemical regime using a satellite-derived photochemical indicator, we are able to compare observed O_3 weekly cycles with corresponding simulation results in order to evaluate model performance. Through the comparison, we are able to understand and even forecast the highest and lowest O_3 anomaly days over the region.

The results of this research warrant future research that addresses several remaining issues. First, our definition of a "chemical regime" is loosely associated with satellite or land use-based characteristics. Besides the inherent uncertainties

Table 5. The number of data (NO_x concentration), the standard deviation, and the standard error of the mean (SEM) of CMAQ simulations with GOME-2 adjusted emissions for NO_x measurement sites over the AVHRR-derived geographical regions and GOME-2-derived chemical regimes.

			2nd CMAQ (NO_x)					2nd CMAQ (NO_x)	
	Day	N	σ	$\sigma N^{-1/2}$		Day	N	σ	$\sigma N^{-1/2}$
Urban	SU	904	5.8	0.2	Saturated	SU	746	6.2	0.2
	MO	748	5.8	0.2		MO	616	6.5	0.3
	TU	554	6.7	0.3		TU	455	7.6	0.4
	WE	556	8.3	0.4		WE	453	9.3	0.4
	TH	749	8.4	0.3		TH	604	8.8	0.4
	FR	751	7.0	0.3		FR	613	7.8	0.3
	SA	886	8.5	0.3		SA	730	8.5	0.3
Others	SU	2940	3.2	0.1	Mixed	SU	2058	3.9	0.1
	MO	2453	4.1	0.1		MO	1665	5.0	0.1
	TU	1790	5.2	0.1		TU	1250	6.0	0.2
	WE	1833	5.8	0.1		WE	1246	6.6	0.2
	TH	2491	5.9	0.1		TH	1700	7.2	0.2
	FR	2516	5.6	0.1		FR	1688	7.1	0.2
	SA	2902	5.1	0.1		SA	2022	5.9	0.1
Forest	SU	1009	3.8	0.1	Sensitive	SU	2370	2.6	0.1
	MO	848	4.4	0.2		MO	2013	2.8	0.1
	TU	635	5.2	0.2		TU	1479	2.9	0.1
	WE	653	5.5	0.2		WE	1530	3.8	0.1
	TH	869	5.6	0.2		TH	2061	3.8	0.1
	FR	855	5.6	0.2		FR	2083	3.6	0.1
	SA	1006	4.6	0.1		SA	2364	4.2	0.1

from satellite retrievals and land use data, the categorization approach used to derive chemical regimes may not collocate with the actual chemical environment in the lower troposphere, where surface ozone is photo-chemically produced. The satellite HCHO and NO_2 columns represent the vertical accumulation of corresponding species from the ground to the top of the troposphere. The use of column data can be justified by the fact that the majority of emission sources of NO_x and VOCs originate at (mobile, area, and biogenic) or near (power plant sources, typically with chimneys in the lower km) the earth's surface. Nevertheless, the potential impact of the vertical distribution of these species, particularly that caused by differences in the chemical lifetime and emission source distribution, on the determination of a chemical regime must also be taken into account. Second, our study is also limited to one month (August 2009). Using a single month for analysis could be problematic in terms of statistics for looking at weekday-weekend differences. Longer-time scale simulations need to average out the impact of synoptic variability on the weekly variations of O_3 and its precursors. As the number of the sampling data increases, the standard error of the mean (SEM) of EPA AQS observations and corresponding simulation results for each day decreases. Therefore, further investigation of changes in the chemical regime over space during other seasons/years could expand our understanding of this phenomenon. Such future investigations would need to determine the chemical environment (e.g., satellite-derived $HCHO/NO_2$ ratios) for each month in order to distinguish the chemical regime stations. In addition, the anthropogenic and biogenic emissions are expected to change from season to season and from year to year in various directions, resulting in a so-called "seasonal transition" of the chemical regime (e.g., Jacob et al., 1995; Martin et al., 2004). While the static land use-based indicator may not capture such seasonal changes, a satellite-based dynamic indicator could more realistically reflect the temporal evolution of the chemical environment.

Acknowledgements. This paper is dedicated to the memory of NOAA ARL Air Quality Group Lead, Daewon Byun (1955–2011), whose leadership and pursuit of scientific excellence continue to inspire us. The authors are grateful to two anonymous reviewers, other members of the NOAA ARL Air Quality Group and NOAA NCEP modeling group members, particularly Rick Saylor and Ariel Stein, for contributing their insightful comments, Fantine Ngan for preparing for chemical boundary conditions, and Jeff McQueen and Ivanka Stajner for their technical input and discussion. We also acknowledge the free use of tropospheric NO_2 and HCHO column data from the GOME-2 sensor from www.temis.nl.

Edited by: J. G. Murphy

References

Anderson, J. R., Hardy, E. E., Roach, J. T., and Witmer, R. E.: A land use and land cover classification system for use with remote sensor data, Geol. Surv. Prof. Paper, 964, 1–28, 1976.

Beirle, S., Platt, U., Wenig, M., and Wagner, T.: Weekly cycle of NO2 by GOME measurements: a signature of anthropogenic sources, Atmos. Chem. Phys., 3, 2225–2232, doi:10.5194/acp-3-2225-2003, 2003.

Bey, I., Jacob, D. J., Yantosca, R. M., Logan, J. A., Field, B. D., Fiore, A. M., Li, Q., Liu, H. Y., Mickley, L. J., and Schultz, M. G.: Global modeling of tropospheric chemistry with assimilated meteorology: Model description and evaluation, J. Geophy. Res., 106, 23073–23095, 2001.

Blanchard, C. L. and Tanenbaum, S.: Weekday/weekend Differences in Ambient Air Pollutant Concentrations in Atlanta and the Southeastern United States, J. Air Waste Manage., 56, 271–284, 2006.

Blanchard, C. L., Tanenbaum, S., and Lawson, D. R.: Differences between Weekday and Weekend Air Pollutant Levels in Atlanta; Baltimore; Chicago; Dallas-Fort Worth; Denver; Houston; New York; Phoenix; Washington, D. C.; and Surrounding Areas, J. Air Waste Manage., 58, 1598–1615, 2008.

Boersma, K. F., Eskes, H. J., and Brinksma, E. J.: Error Analysis for Tropospheric NO_2 retrieval from Space, J. Geophys. Res., 109, D04311, doi:10.1029/2003JD003962, 2004.

Choi, Y., Wang, Y., Zeng, T., Cunnold, D., Yang, E., Martin, R., Chance, K., Thouret, V., and Edgerton, E.: Springtime transitions of NO_2, CO, and O_3 over the North America: Model evaluation and analysis, J. Geophys. Res., 113, D20311, doi:10.1029/2007JD009632, 2008.

Choi, Y., Kim, J., Eldering, A., Osterman, G., Yung, Y. L., Gu, Y., and Liou, K. N.: Lightning and anthropogenic NO_x sources over the United States and the western North Atlantic Ocean: Impact on OLR and radiative effects, Geophys. Res. Lett., 36, L17806, doi:10.1029/2009GL039381, 2009.

Cleveland, W. S., Graedel, T. E., Kleiner, B., and Warner, J. L: Sunday and Workday Variations in Photochemical Air Pollutants in New Jersey and New York, Science, 186, 1037–1038, 1974.

De Smedt, I., Müller, J.-F., Stavrakou, T., van der A, R., Eskes, H., and Van Roozendael, M.: Twelve years of global observations of formaldehyde in the troposphere using GOME and SCIAMACHY sensors, Atmos. Chem. Phys., 8, 4947–4963, doi:10.5194/acp-8-4947-2008, 2008.

Duncan, B. N., Yoshida, Y., Olson, J. R., Sillman, S., Martin, R. V., Lasmal, L., Hu, Y., Pickering, K. E., Retscher, C., Allen, D. J., and Crawford, J. H.: Application of OMI observations to a space-based indicator of NO_x and VOC controls on surface ozone formation, Atmos. Environ., 44, 2213–2223, 2010.

Elkus, B. and Wilson, K. R.: Photochemical air pollution: Weekend-weekday difference, Atmos. Envion., 11, 509–515, 1977.

Foley, K. M., Roselle, S. J., Appel, K. W., Bhave, P. V., Pleim, J. E., Otte, T. L., Mathur, R., Sarwar, G., Young, J. O., Gilliam, R. C., Nolte, C. G., Kelly, J. T., Gilliland, A. B., and Bash, J. O.: Incremental testing of the Community Multiscale Air Quality (CMAQ) modeling system version 4.7, Geosci. Model Dev., 3, 205–226, doi:10.5194/gmd-3-205-2010, 2010.

Fujita, E. M., Stockwell, W. R., Campbell, D. E., Keisiar, R. E., and Lawson, D. R.: Evolution of the magnitude and spatial extend of the weekend ozone effect in California's South Coast Air Basin, 1981–2000, J. Air Waste Manage., 53, 801–815, 2003.

Houyoux, M. R., Vulkovich, J. M., Coats, C. J., Wheeler, N. M., and Kasibhatla, P. S.: Emission inventory development and processing for the Seasonal Model for Regional Air Quality (SMRAQ) project, J. Geophy. Res., 105, 9079–9090, 2000.

Jacob, D. J., Horowitz, L. W., Munger, J. W., Heikes, B. G., Dickerson, R. R., Artz, R. S., and Keene, W. C.: Seasonal transition from NO_x- to hydrocarbon-limited conditions for ozone production over the eastern United States in September, J. Geophys. Res., 100, 9315–9324, 1995.

Kaynak, B., Hu, Y., Martin, R. V., Sioris, C. E., and Russell, A. G.: Comparison of weekly cycle of NO_2 satellite retrievals and NO_x emission inventories for the continental United States, J. Geophys. Res., 114, D05302, doi:10.1029/2008JD010714, 2009.

Kim, S.-W., Heckel, A., Frost, G. J., Richter, A., Gleason, J., Burrows, J. P., McKeen, S., Hsie, E. Y., Granier, C., and Trainer, M: NO_2 columns in the western United States observed from space and simulated by a regional chemistry model and their implications for NO_x emissions, J. Geophys. Res., 114, D11301, doi:10.1029/2008JD011343, 2009.

Lamsal, L. N., Martin, R. V., van Donkelaar, A., Steinbacher, M., Celarier, E. A., Bucesela, E., Dunlea, E. J., and Pinto, J. P.: Ground-level nitrogen dioxide concentrations inferred from the satellite-borne Ozone Monitoring Instrument, J. Geophys. Res., 113, D16308, doi:10.1029/2007JD009235, 2008.

Lebron, F.: A comparison of weekend-weekday ozone and hydrocarbon concentrations in the Baltimore-Washington metropolitan area, Atmos. Environ., 9, 861–863, 1967.

Lee, P. and Ngan, F.: Coupling of important physical processes in the Planetary Boundary Layer between Meteorological and Chemistry Models for Regional to Continental Scale Air Quality Forecasting: An Overview, Atmosphere, 2, 464–483, 2011.

Loveland, T. R., Reed, B. C., Brown, J. F., Ohlen, D. O., Zhu, J., Yang, L., and Merchant, J. W.: Development of a Global Land Cover Characteristics Database and IGBP DISCover from 1-km AVHRR Data, Int. J. Remote Sens., 21, 1303–1330, 2000.

Marr, L. C. and Harley, R. A.: Spectral analysis of weekday-weekend differences in ambient ozone, nitrogen oxide, and non-methane hydrocarbon time series in California, Atmos. Environ., 36, 2327–2335, 2002.

Martin, R. V., Jacob, D. J., Chance, K., Kurosu, T. P., Palmer, P. I., and Evans, M. J.: Global inventory of nitrogen oxide emissions constrained by space-based observations of NO_2 columns, J. Geophys. Res., 108, 4537, doi:10.1029/2003JD003453, 2003.

Martin, R. V., Fiore, A., and Van Donkelaar, A.: Space-based diagnosis of surface ozone sensitivity to anthropogenic emissions, Geophys. Res. Lett., 31, L06120, doi:10.1029/2004GL019416, 2004.

Martin, R. V., Sioris, C. E., Chance, K., Ryerson, T. B., Bertram, T. H., Wooldridge, P. J., Cohen, R. C., Neuman, J .A., Swanson, A., and Flocke, F. M.: Evaluation of space-based constraints on global nitrogen oxide emissions with regional aircraft measurements over and downwind of eastern North America, J. Geophys. Res., 111, D15308, doi:10.1029/2005JD006680, 2006.

Napelenok, S. L., Pinder, R. W., Gilliland, A. B., and Martin, R. V.: A method for evaluating spatially-resolved NO_x emissions using Kalman filter inversion, direct sensitivities, and space-based NO_2 observations, Atmos. Chem. Phys., 8, 5603–5614, doi:10.5194/acp-8-5603-2008, 2008.

Qin, Y., Tonnesen, G. S., and Wang, Z.: Weekend/weekday differences of ozone, NO_x, CO, VOCs, PM_{10} and the light scatter during ozone season in southern California, Atmos. Environ., 38, 3069–3087, 2004.

Russell, A. R., Valin, L. C., Bucsela, E. J., Wenig, M. O., and Cohen, R. C.: Space-based constraints on spatial and temporal patterns of NO_x emissions in California, 2005–2008, Environ. Sci. Tech., 44, 3608–3615, doi:10.1021/es903451j, 2010.

Shutters, S. T. and Balling Jr., R. C.: Weekly periodicity of environmental variables in Phoenix, Arizona, Atmos. Envion., 40, 304–310, 2006.

Sillman, S.: The relation between ozone, NO_x and hydrocarbons in urban and polluted rural environments, Atmos. Envion., 33, 1821–1845, 1999.

Sillman, S., Jennifer, A. L., and Wofsy, S. C.: The Sensitivity of Ozone to Nitrogen Oxides and Hydrocarbons in Regional Ozone Episodes, J. Geophys. Res., 95, 1837–1851, 1990.

Tang, Y., Lee, P., Tsidulko, M., Huang, H. C., McQueen, J. T., Dimego, G. J., Emmons, L. K., Pierce, R. B., Thompson, A. M., Lin, H., Kang, D., Tong, D., Yu, S., Mathur, R., Pleim, J. E., Otte, T. L., Pouliot, G., Young, J. O., Schere, K. L., Davison, P. M., and Stajner, I.: The impact of chemical lateral boundary conditions on CMAQ predictions of tropospheric ozone over the continental United States, Environ. Fluid Mech., 9, 43–58, doi:10.1007/s10652-008-9092-5, 2008.

Tong, D. Q. and Mauzerall, D. L.: Spatial variability of summertime tropospheric ozone over the continental United States: Implications of an evaluation of the CMAQ model, Atmos. Environ., 40, 3041–3056, 2006.

Vukovich, F. M.: The spatial variation of the weekday/weekend differences in the Baltimore area, J. Air Waste Manage., 50, 2067–2072, 2000.

Yarwood, G., Grant, J., Koo, B., and Dunker, A. M.: Modeling weekday to weekend changes in emissions and ozone in the Los Angeles basin for 1997 and 2010, Atmos. Environ., 42, 3765–3779, 2008.